Spatiotemporal organization of Aurora-B by APC/C^{Cdh1} after mitosis coordinates cell spreading through FHOD1

Suzanne Floyd[1,§§], Nicola Whiffin[1,*,§§], Maria P. Gavilan[1,‡], Stefan Kutscheidt[2], Maria De Luca[1,§], Chiara Marcozzi[1,¶], Mingwei Min[1], Johnathan Watkins[1,], Kathryn Chung[1,‡‡], Oliver T. Fackler[2] and Catherine Lindon[1,¶¶]**

[1]University of Cambridge Department of Genetics, Downing Street, Cambridge CB2 3EH, UK
[2]Department of Infectious Diseases, Virology, University Hospital Heidelberg, Im Neuenheimer Feld 324, 69120 Heidelberg, Germany

*Present address: Genetics and Epidemiology, Institute of Cancer Research, Sutton SM2 5NG, UK
‡Present address: Cell Signalling Department, CABIMER-CSIC, 41092-Seville, Spain
§Present address: Department of Biological and Environmental Sciences and Technologies (DiSTeBA), University of Salento, 73100 Lecce, Italy
¶Present address: Gurdon Institute and University of Cambridge Department of Zoology, Downing St., Cambridge CB2 3EJ, UK
**Present address: Breakthrough Breast Cancer Unit, Research Oncology, King's College London SE1 9RT, UK
‡‡Present address: Ludwig Institute for Cancer Research, University of Oxford, Nuffield Department of Clinical Medicine, OX3 7DQ, UK
§§These authors contributed equally
¶¶Author for correspondence (c.lindon@gen.cam.ac.uk)

Accepted 2 April 2013
Journal of Cell Science 126, 2845–2856

doi: 10.1242/jcs.123232

Summary

Spatiotemporal regulation of mitotic kinase activity underlies the extensive rearrangement of cellular components required for cell division. One highly dynamic mitotic kinase is Aurora-B (AurB), which has multiple roles defined by the changing localisation of the chromosome passenger complex (CPC) as cells progress through mitosis, including regulation of cytokinesis and abscission. Like other mitotic kinases, AurB is a target of the anaphase-promoting complex (APC/C) ubiquitin ligase during mitotic exit, but it is not known if APC/C-mediated destruction plays any specific role in controlling AurB activity. We have examined the contribution of the Cdh1 coactivator-associated APC/C^{Cdh1} to the organization of AurB activity as cells exit mitosis and re-enter interphase. We report that APC/C^{Cdh1}-dependent proteolysis restricts a cell-cortex-associated pool of active AurB in space and time. In early G1 phase this pool of AurB is found at protrusions associated with cell spreading. AurB retention at the cortex depends on a formin, FHOD1, critically required to organize the cytoskeleton after division. We identify AurB phosphorylation sites in FHOD1 and show that phosphomutant FHOD1 is impaired in post-mitotic assembly of oriented actin cables. We propose that Cdh1 contributes to spatiotemporal organization of AurB activity and that organization of FHOD1 activity by AurB contributes to daughter cell spreading after mitosis.

Key words: Aurora kinase B, APC/C-mediated proteolysis, FHOD1, Mitotic exit

Introduction

Cells preparing to divide undergo extensive rearrangement of the cytoskeleton that include loss of integrin-mediated adhesion, disassembly of actin structures and cell rounding (Kunda and Baum, 2009). As cells exit mitosis to return to interphase these processes are reversed. Very little is known about how such events are regulated, but in common with other steps of mitotic exit, they are assumed to require reversals of specific mitotic phosphorylation events that depend on upregulation of phosphatase activity and/or inactivation of mitotic kinases (Wurzenberger and Gerlich, 2011).

Ubiquitin-mediated proteolysis is one route to inactivation of mitotic kinases. The anaphase-promoting complex (APC/C) ubiquitin ligase targets a large number of substrates at mitotic exit (Pines, 2011) including mitotic kinases that play essential roles during mitotic exit, most notably Plk1 and AurB (Lindon and Pines, 2004; Stewart and Fang, 2005). Perturbing degradation of these kinases perturbs mitotic exit (Floyd et al., 2008; Lindon and Pines, 2004; Stewart and Fang, 2005), consistent with the idea that ubiquitin-mediated proteolysis can contribute to dynamic spatial redistribution of kinase activity through targeting of specific subpopulations (Lindon, 2008).

The multiple essential roles of AurB require repeated relocalisation of the kinase during mitosis (Carmena and Earnshaw, 2003). AurB is the enzymatic core of the CPC and depends on other members of the complex (notably INCENP) for localisation and activity. At anaphase CPC relocalises to the spindle midzone, with AurB playing critical roles in promoting assembly of the midzone and in signalling to the equatorial cortex to trigger cytokinesis (Douglas et al., 2010; Hümmer and Mayer, 2009). After anaphase the spindle midzone is compacted into the midbody matrix and AurB activity at the midbody regulates timing of abscission (Steigemann et al., 2009). AurB has specific target interactors and substrates during mitotic exit, including known regulators of cytokinesis and abscission (Bastos et al., 2012; Capalbo et al., 2012; Douglas et al., 2010; Neef et al., 2006) and others identified via proteomic studies whose function in mitotic exit is unknown (Ozlü et al., 2010). One such interactor

is the diaphanous-related formin (DRF), formin homology 2 (FH2) domain-containing protein 1 (FHOD1). Formins nucleate actin filaments by stabilizing actin dimers through the conserved FH2 domain and promote their elongation by capping the barbed end of growing filaments. DRFs have also been found to regulate microtubule (MT) dynamics independent of their actin nucleation function (Bartolini et al., 2008; Cheng et al., 2011) and are increasingly recognized as mediators of interactions between MT and actin cytoskeletons (Bartolini and Gundersen, 2010; Chesarone et al., 2010).

In addition to specific roles for AurB in promoting mitotic exit, pathways attenuating AurB activity are also required for different steps in mitotic exit (Ramadan et al., 2007; Sumara et al., 2007; Vázquez-Novelle and Petronczki, 2010; Wurzenberger et al., 2012). However, the targeted destruction of AurB by the APC/C has not yet been shown to play any specific role in controlling AurB activity during mitotic exit. Here we have tested the idea that APC/C contributes to dynamic spatial organization of AurB activity as cells return to interphase. We uncover a role for Cdh1-dependent APC/C activity in controlling a subpopulation of AurB that is recruited to the cell cortex in a FHOD1-dependent manner in early G1 phase to play a role in promoting post-mitotic spreading via FHOD1.

Results

APC/C^{Cdh1} exerts spatial control on AurB kinase activity at the end of mitosis

Previous studies have indicated that, at the end of mitosis, AurB disappears from the cell later than other APC/C substrates (Floyd et al., 2008; Lindon and Pines, 2004; Sigl et al., 2009), and indeed *in vivo* time-lapse analysis of AurB–GFP degradation reveals Cdh1-dependent proteolysis of AurB continuing over a window of time that extends well into G1 phase (C.M., M.M. and C.L., unpublished data). We wanted to test the idea that ongoing AurB proteolysis contributes to the organization of mitotic exit. Therefore we examined the distribution of AurB at early G1 phase in synchronized, fixed populations of human HeLa, hTERT-RPE1 (RPE) and U2OS cells after brief treatment with the proteasome inhibitor MG132 or after siRNA-mediated silencing of Cdh1 expression (Fig. 1A–E; supplementary material Fig. S1 and data not shown). As expected we found most cellular AurB at the midbody, and in siRNA-treated (Cdh1-i) cells there was also some accumulation of AurB in the nucleus. In addition, we noticed in approximately half of MG132-treated or Cdh1-i cells a small population of AurB localised at the edge of the cell at sites distal to the midbody (Fig. 1A,B; supplementary material Fig. S1). We confirmed that other CPC components (INCENP, survivin) colocalised with AurB at these sites (supplementary material Fig. S1). In some cells these sites appeared to correspond to the cortical extremities of MTs (Fig. 1A,E). In other cells AurB colocalised with actin-rich structures (supplementary material Fig. S1), as previously reported during monopolar cytokinesis (Hu et al., 2008) or in cells overexpressing AurB–GFP (Abdullah et al., 2005), indicating that AurB might be able to interact with either MTs or F-actin at different times or under different conditions.

Next, we tested if this cortical pool of AurB contained active kinase, using a phospho-specific antibody raised against AurB phospho-T232 (pAur). The midbody stained strongly with pAur antibody in most control and Cdh1-i cells. In addition we found that the population of AurB at the cell cortex, but not that in the nucleus, also stained with the pAur antibody (Fig. 1C). We measured the intensity of staining with pAur and AurB antibodies at different locations in the cell to obtain an estimate of relative state of activity of AurB (Fig. 1D; supplementary material Fig. S1). We found that whereas chromatin-associated AurB did not stain with pAur, consistent with phosphatase-mediated inactivation of this pool (Murnion et al., 2001; Vagnarelli et al., 2011), relative AurB kinase activity at the cell edge in either control or Cdh1-i cells appeared almost as high as in the midbody. In conclusion, active AurB is present at the cell cortex in early G1 phase and is readily detectable under conditions where it is not degraded efficiently during mitotic exit.

We also found AurB at the cell cortex in a fraction of early G1 cells that had not been treated with Cdh1-i or MG132 (Fig. 1B). This early G1 window (during which daughter cells remain connected via a midbody-containing intercellular bridge) typically lasts an hour or more. Since even brief treatment with MG132 significantly increased the fraction of cells showing cortical AurB we hypothesized that AurB localisation to the cell edge was a transient event occurring in all early G1 phase cells. Indeed, approximate staging of our populations of fixed cells indicated that cortical AurB was systematically associated with 'young' G1 cells but absent from those with a more mature intercellular bridge (Fig. 1E). To test our hypothesis, we created a cell line expressing Venus-tagged AurB under tight tetracycline control, suitable for dynamic study of AurB localisation in living cells (Fig. 1F–H). AurB–Venus mimicked faithfully the enrichment of endogenous AurB to the cell edge seen in fixed populations of G1 phase cells (Fig. 1G–H). Moreover, a version of AurB–Venus lacking the N-terminal KEN motif (Nguyen et al., 2005) that is partially stabilized during mitotic exit (C.M., M.M. and C.L., unpublished data) was more frequently found in this localisation, confirming that proteolysis of AurB–Venus defines the fraction of cells showing cortical localisation of the kinase (Fig. 1H). In time-lapse analyses of living cells we found that AurB–Venus did indeed localise to the edge of the cell in a spatially and temporally restricted manner. Cortical enrichments of AurB–Venus appeared in almost every cell analysed (89.7%, $n=39$), during a time window beginning 15 ± 3 minutes after anaphase onset and lasting for 33 ± 9 minutes (Fig. 1F; Fig. 2A; Table 1), and systematically associated with protrusions of the cell cortex that occur during post-mitotic spreading (supplementary material Movie 1). Therefore AurB recruitment to the cell edge is an event that occurs during a specific window of time during mitotic exit.

Localisation of AurB to the cell cortex is dependent on MTs and the actin cytoskeleton

To define parameters involved in spatiotemporal regulation of AurB in early G1 we examined the dynamics of AurB–Venus localisation when proteolysis was inhibited, by adding MG132 to cells during filming. We found that the timing of appearance of AurB–Venus at the cell cortex was unchanged, but that the kinase accumulated all along the spreading edge of early G1 cells (Fig. 2B; supplementary material Movie 2) and persisted there, frequently until the end of filming ($\geq87\pm21$ minutes in MG132, Fig. 2A; Table 1). We concluded that removal of the kinase from the cell cortex is proteolysis-dependent. Next we examined the role of cytoskeletal components in localising AurB to the cell cortex. Treatment of cells with the MT depolymerizing drug nocodazole shortly after anaphase onset prevented AurB–Venus localisation to the cell cortex (Fig. 2A,B; supplementary material

Movie 3). Consistently, treatment with the MT stabilizing agent taxol induced strong accumulation of AurB–Venus on cortical MT bundles (Fig. 2A,B). In contrast, disruption of F-actin by treatment with cytochalasin D increased the persistence of AurB–Venus spots visible near the cell edge (Fig. 2A,B). Inhibition of Aurora B kinase activity by addition of the inhibitor ZM447439 (ZM) (Ditchfield et al., 2003) reduced recruitment of AurB–Venus to the cell cortex (Fig. 2A), which could explain why AurB is not seen at the cortex in MG132-treated interphase cells, when it is not fully active. Together we interpreted these data to mean that active AurB travels to the early G1 cell cortex on MTs but is then removed from them in a manner that depends on

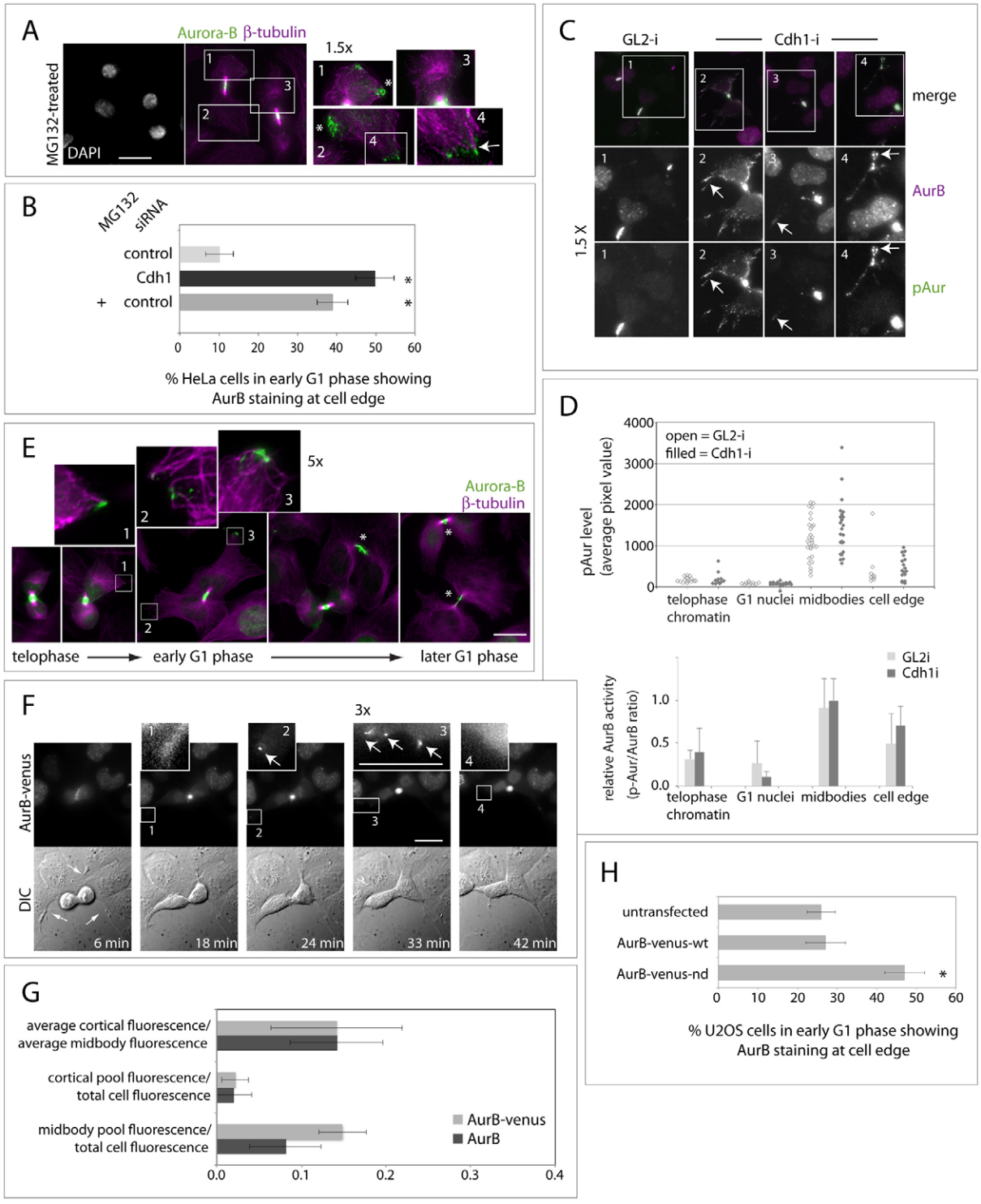

Fig. 1. See next page for legend.

F-actin, and retained at the cortex in a manner limited by ubiquitin-mediated proteolysis.

APC/C^{Cdh1} regulates the actin cytoskeleton in early G1 phase through targeting of AurB

We investigated the role of the newly characterized cortical pool of AurB in post-mitotic spreading of daughter cells, a process that requires coordination of MT and actin networks in early G1 phase. We used RPE cells for this study, since these spread rapidly after division, showing marked polarization in early G1 phase. For time-lapse observation of actin organization in living cells we used Venus-tagged α-actinin to label the actin cytoskeleton, allowing visualization of stress fibres (SFs), focal adhesion complexes and other actin-rich structures (Edlund et al., 2001). We generated a stable cell line, RPE-α-actinin–Venus, in which daughter cells show strongly polarized spreading after division, such that protrusive activity occurs at the furthest point from the site of division (supplementary material Movie 4). This protrusive activity usually establishes a single leading edge per cell at a site distal to the intercellular bridge. Daughter cells then migrate away from each other, typically with a persistent directionality determined by the position of cleavage (Albrecht-Buehler, 1977) that maximizes the distance between them during early G1 (supplementary material Fig. S2). SFs become visible, either as dorsal fibres behind the leading edge or as lateral peripheral fibres, ~45 minutes after anaphase onset (Fig. 2C,D).

We treated RPE-α-actinin–Venus cells with MG132 shortly after anaphase onset and found that proteolysis inhibition during mitotic exit prevented polarized cell spreading and significantly delayed re-assembly of SFs at the end of mitosis (Fig. 2C,D). At least some of this effect was the result of stabilizing substrates of APC/C^{Cdh1} because we saw a similar effect in Cdh1-i cells. Cdh1-i cells displayed continuous ruffling and short-lived protrusions all around the edge of daughter cells, were slow to adopt a polarized shape (Fig. 2C,E; supplementary material Movie 5), failed to establish a clear leading edge and showed reduced directionality in migration (supplementary material Fig. S2). The timing of α-actinin–Venus recruitment to sites of cortical activity and in focal adhesions appeared normal (17±5 minutes and 18±5 minutes respectively, $n=16$), while the appearance of SFs was delayed (63.3±23 versus 44.9±11 for control cells, $P<0.01$ by Student's t-test; Fig. 2D). In particular we observed in Cdh1-i cells an absence of SFs along the cell periphery. We concluded that proteolysis of one or more Cdh1 targets contribute to reassembly of SFs and to polarized cell shape at the start of interphase.

We then tested if one of these targets was AurB, by treating control and Cdh1-i cells with ZM shortly after anaphase entry to test if we could accelerate assembly of SFs through inhibition of AurB. We found that ZM treatment did significantly accelerate the appearance of SFs in control cells (Fig. 2C,D). In Cdh1-i cells, however, this effect was less consistent and moreover loss of cell shape was only partially rescued by AurB inhibition (Fig. 2C–E). Instead, ZM treatment produced immediate pronounced ruffling and extension of existing lamellipodia-like protrusions (Fig. 2C, supplementary material Movie 6). It is possible that ZM is added too late in these experiments to influence cell polarity (it cannot be added earlier than late telophase without causing cytokinesis to fail) and also likely that the effects of Cdh1-i depend on additional targets, such as Rho regulators p190rhoGAP and Ect2 (Liot et al., 2011; Naoe et al., 2010). We also reasoned that cell-wide inhibition of AurB might not be able to rescue effects on cell spreading that depend on spatial organization of AurB activity.

AurB is recruited to the cell cortex by FHOD1

To understand more about the spatial organization of AurB in mitotic exit we tested known AurB interactors that might contribute to its distinctive localisation during mitotic exit. These included the C-(cytokinesis)-phase-specific AurB interactor FHOD1 (Ozlü et al., 2010), which seemed a particularly promising candidate for an interactor defining a distinct pool of AurB, since in our experiments – unlike other documented interactors – it appeared to be absent from the midbody. Moreover, FHOD1 had previously been implicated in driving cell elongation in human tissue culture cells (Gasteier et al., 2005).

Fig. 1. Spatiotemporal control of AurB kinase activity by APC/C^{Cdh1} in early G1 phase. (**A–D**) Synchronized populations of HeLa cells were fixed 13 hours after release from thymidine/aphidicolin block and stained for AurB and tubulin (A,B) or pAur and AurB (C,D). (A) Representative images of cells treated for 15 minutes with 4 μM MG132. Enlarged images of the boxed regions are shown in which the brightness and contrast have been adjusted to reveal AurB at the cell cortex; all pixels within insets were treated in an identical fashion. AurB appears to colocalise with MT tips in some areas (arrow) but not in others (asterisks). (B) Quantification of AurB localisation in early G1 cells of populations treated with GL2 (control) or Cdh1 siRNA, or with MG132 as in A. Early G1 phase is defined as the window of time during which daughter cells are attached by an AurB-positive midbody. At least 100 cells were scored for each condition in five or more separate experiments, and mean values plotted as bar graphs with standard deviations (s.d.) shown. *$P<0.001$, χ^2-test. (C) Representative images of siRNA-treated populations stained for AurB and pAur. Enlarged images of the boxed regions are shown, in which the brightness and contrast have been adjusted, and all pixels treated in an identical fashion. Arrows indicate cortical pAur/AurB staining. Specificity of pAur antibody is confirmed in supplementary material Fig. S1. (D) Distribution of active AurB, using average pAur and AurB pixel values measured in different regions of cells stained as in C, corrected for background value adjacent to each cell. Upper panel shows distribution of individual pAur values. Bar graphs show the ratio of pAur/AurB values (means ± s.d., normalized to the maximum value, which was set to 1.0) to indicate the relative activity of each pool of AurB. See also supplementary material Fig. S1. (**E–H**) Validation of AurB–Venus as a marker for a cortical pool of AurB. (E) Approximate staging of untreated U2OS cells in early G1, fixed and stained to reveal endogenous AurB. Enlarged images of the boxed regions show AurB staining at the cell cortex in 'younger' daughter cells; asterisks indicate midbodies of presumed 'older' daughters where no cortical AurB is detectable. (F) Time-lapse fluorescence imaging of mitotic exit in U2OS cell expressing AurB–Venus. Images are frames from supplementary material Movie 1, shown as maximum intensity projections of 1 μm stacks, with times adjusted to anaphase onset. Brightness and contrast have been adjusted within the enlarged boxed regions, with each pixel of the inserts treated in an identical fashion. Arrows on first of DIC series indicate the position of retraction fibres at metaphase. See also Fig. 2A and Table 1. (**G**,**H**) Comparison of AurB localisation in U2OS cells fixed and stained for AurB as in E, with AurB–Venus localisation in U2OS-AurB–Venus cells fixed and stained with GFP antibody. (G) AurB or GFP pixel values measured in the cortical pool were expressed as a fraction of midbody or total fluorescence, after correction for background pixel values. Bar graphs show mean values ± s.d. of ratios measured in at least 10 cells from two separate experiments. (H) Localisation to the cell cortex of endogenous AurB in U2OS cells and AurB–Venus-wt or AurB–Venus lacking the N-terminal KEN motif AurB-Venus-nd in cell lines were scored as described in B. Scale bars: 20 μm.

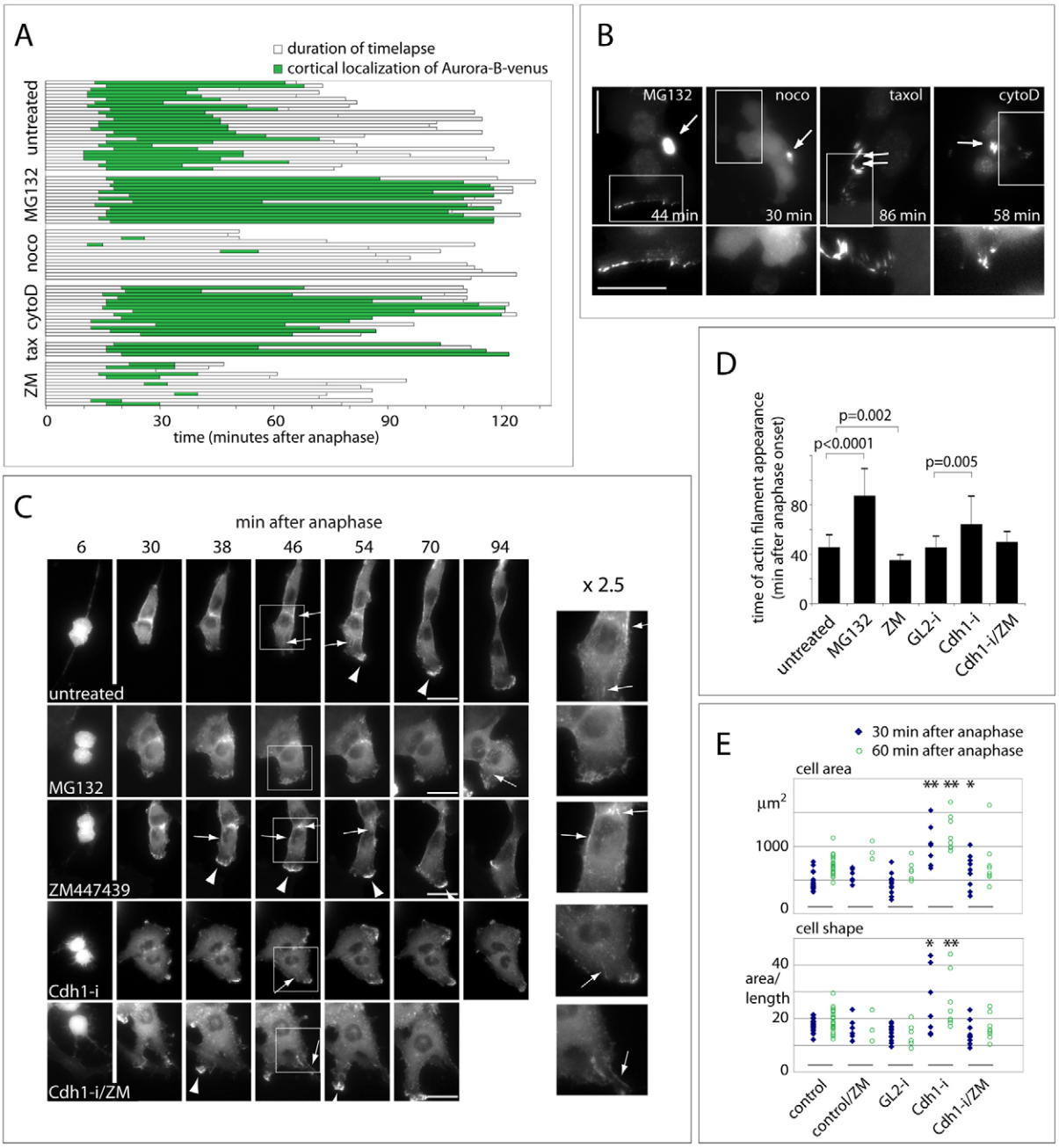

Fig. 2. Cdh1 and AurB kinase influence cell spreading in early G1. (**A**,**B**) U2OS-AurB–Venus cells were treated with the indicated drugs after anaphase onset (doses in Materials and Methods) and recorded by time-lapse microscopy as in Fig. 1F. (A) Results from multiple experiments plotted as bars representing trajectories of individual cells. A statistical summary of these data can be found in Table 1. (B) Frames from representative movies with times adjusted to anaphase onset. Drug treatments occurred at the following times after anaphase for the cells shown: MG132 (13 minutes), nocodazole (noco; 8 minutes), taxol (10 minutes), cytochalasin D (cytoD; 8 minutes). Brightness and contrast have been adjusted in the enlarged images of the boxed regions to show AurB accumulation (or lack thereof) at the edge of the cell. Arrows indicate midbodies. (**C**) Representative frames from fluorescence time-lapse microscopy of non-confluent cell cultures of RPE-α-actinin–Venus, with the appearance of α-actinin-associated structures scored by arrows (actin fibres) or arrowheads (leading edges). The images on the right are enlargements of the 46 minutes time point. See supplementary material Movies 4–6. Drugs, as indicated, were added at the following times after anaphase onset: MG132, 8 minutes; ZM, 10 minutes; Cdh1i/ZM, 17 minutes. (**D**) The timings of actin fibre assembly using time-lapse data collected during two or more experiments and plotted as means ± s.d. *P*-values were calculated using Student's *t*-test. (**E**) Time-lapse movies of RPE-α-actinin–Venus cells were used to measure the area of daughter cells during cell spreading (upper panel). Length of daughter cells was measured from midbody to cell edge along the axis defined by the position of the anaphase spindle and a cell shape index calculated by expressing the cell area as a function of cell length (lower panel). Distribution of measurements from individual cells are shown: elongated, polarized daughter cells give the lowest cell shape index. **P*<0.01, ***P*<0.001, Student's *t*-test. Scale bars: 20 μm.

Table 1. Statistical analysis of AurB–Venus localisation data shown in Fig. 2A

Treatment	First appearance (minutes after anaphase)	Duration (minutes)	*P*-value versus untreated (Student's *t*-test)	Number of cells analysed	Number of cells with no AurB at cell edge
Untreated	15.0±3.4	33±9.2		20	2
MG132	16.8±2.9	87±21*	<0.0001	14	0
Nocodazole	24.7±13.6	6.7±3.1	<0.01	15	12
ZM447439	19.5±7.4	13±6.8	<0.0001	14	6
Cytochalasin D	18.5±4.7	66±25*	<0.0001	15	0

*Underestimate.

The available antibody against FHOD1 did not recognize endogenous FHOD1 by immunofluorescence but we found some colocalisation of HA-tagged FHOD1 with AurB–Venus and pAurB at sites at the cell periphery in early G1 phase (Fig. 3A). After siRNA-mediated knockdown of FHOD1 expression (FHOD1-i), we found that AurB–Venus localisation to protrusions of spreading cells was either abolished (52/90 cells from three separate experiments) or attenuated (≤14 minutes in 16/90 cells; Fig. 3B; supplementary material Movies 7, 8). Cortical localisation of AurB was partially rescued by co-transfection of siRNA-resistant RFP-FHOD1 (supplementary material Fig. S3). We also found that localisation of endogenous AurB to the cell periphery in early G1 phase was abolished in FHOD1-i, and rescued by siRNA-resistant FHOD1 (supplementary material Fig. S3). We concluded that FHOD1 is required to maintain a pool of AurB at the cell cortex in early G1 phase.

FHOD1 coordinates MT and actin cytoskeletons during cell spreading

We next examined whether FHOD1 was required for cell spreading in RPE-α-actinin–Venus cells and found pronounced effects on cell shape in FHOD1-i cells after mitosis. Cells spread rapidly but did not do so in correctly polarized fashion, displaying multiple sites of sustained cortical ruffling in early G1 phase (Fig. 3C; supplementary material Movie 9) and, as in Cdh1-i cells, failure to develop a leading edge or to adopt the elongated shape typical of RPE cells (Fig. 3D). We also examined the distribution of F-actin in paraformaldehyde (PFA)-fixed populations of U2OS cells by phalloidin staining, observing in FHOD1-i-treated cells an absence of the robust peripheral actin cables characteristic of control post-mitotic cells (Fig. 3E, see also Fig. 4D). The absence of these cortical actin cables was directly related to loss of cell shape (Fig. 3F). Since cell shape and polarity are generally defined by cues delivered by MTs, we examined the MT network in methanol-fixed populations of U2OS cells and found that the density and organization of the MT network in early G1 cells was reduced after FHOD1-i (Fig. 3G). We noted the absence of MTs oriented along the long axis of the cell and that are required to drive cell elongation (Picone et al., 2010). This population of MTs could be rescued by co-expression of siRNA-resistant HA–FHOD1wt, along with rescue of cell shape (Fig. 3G,H). A version of HA–FHOD1 lacking the FH2 domain (shown to mediate MT stabilization in related formin mDia2) (Bartolini et al., 2008) was not able to rescue (Fig. 3G,H). We then stained U2OS and RPE cells with MT plus-end (+TIP) marker EB3, to examine the presence of +TIPs at the cell cortex. We found that the number of EB3 comets close to the cell cortex was reduced in FHOD1-i (Fig. 3I; supplementary material Fig. S3), consistent with a role for FHOD1 in promoting MT growth to the cell cortex in early G1 cells. In the same experiment we found the density of EB3 comets close to the cortex was increased after treatment of cells with ZM, indicating that AurB activity at this time would generally act to suppress MT growth at the cortex. AurB is known to selectively destabilize MTs at incorrectly attached kinetochores, earlier in mitosis, through recruitment of the kinesin-13 MCAK (Cimini et al., 2006; Knowlton et al., 2006) and MCAK localised to +TIPs close to the cell cortex in early G1 cells (data not shown). We thus propose that AurB and FHOD1 contribute respectively to the selective destabilization and stabilization of MTs required to establish a polarised network in early G1 phase.

AurB controls cell spreading through FHOD1

Finally, we investigated whether FHOD1 is a downstream target of AurB in regulating cell spreading. AurB-dependent phosphorylation (RphosSL, AurB consensus sequence) of FHOD1 had previously been reported (Ozlü et al., 2010). To identify AurB phosphorylation sites in FHOD1 we subjected *in vitro*-phosphorylated full-length FHOD1 to mass spectrometry (supplementary material Fig. S4). Multiple AurB phosphorylation targets were identified in FHOD1 including Ser367 as initially reported (Ozlü et al., 2010) and an additional cluster of four phospho-Ser/Thr residues (between 486 and 498) within the coiled-coil domain that lies just upstream of the conserved FH1 and FH2 domains (Fig. 4A). Since a recent proteomic study confirms that this phosphorylation cluster is present on FHOD1 in mitotic cells (Kettenbach et al., 2011) and these four sites together with Ser367 comprise the large majority of all AurB phospho-sites in FHOD1 (supplementary material Fig. S4), we mutated these five residues to generate phospho-mimetic (FHOD1-5D) or non-phosphorylatable (FHOD1-5A) versions of FHOD1. Expression and immuno-isolation of HA-tagged versions of FHOD1 from human cells confirmed that these five sites (S367, S486, T489, T495, S498) contribute significantly to phosphorylation of FHOD1 by AurB *in vitro* (Fig. 4B,C). To investigate the role of FHOD1 phosphorylation by AurB in cell spreading we carried out siRNA-rescue experiments using the 5D and 5A versions of HA–FHOD1. We used PFA-fixed populations of cells, to examine together actin and MT cytoskeletons and HA–FHOD1 localisation, and MEOH fixation to examine AurB localisation at the cell cortex. We found that AurB recruitment to the cortex was not affected by our phospho-site mutations in FHOD1 (supplementary material Fig. S3). However, we found clear differences in organization of the peripheral cytoskeleton between cells rescued with phospho-mimetic and non-phosphorylatable versions of HA–FHOD1

(Fig. 4D–G). Examination of cells rescued with wild-type HA–FHOD1 revealed, as expected, assembly of peripheral actin SFs in early G1 phase, closely aligned with MTs oriented along the cortex (Fig. 4D left-hand panels, compare HA-positive cell with adjacent non-rescued cell in early G1 phase). We also noted that HA–FHOD1wt itself showed colocalisation with peripheral actin SFs/MTs, and additionally localised to the tips of some MTs at the leading edges of the cell (Fig. 4D,F). The phospho-mimetic HA–FHOD1-5D was able to rescue the assembly of robust peripheral SFs in early G1 phase and showed similar localisation

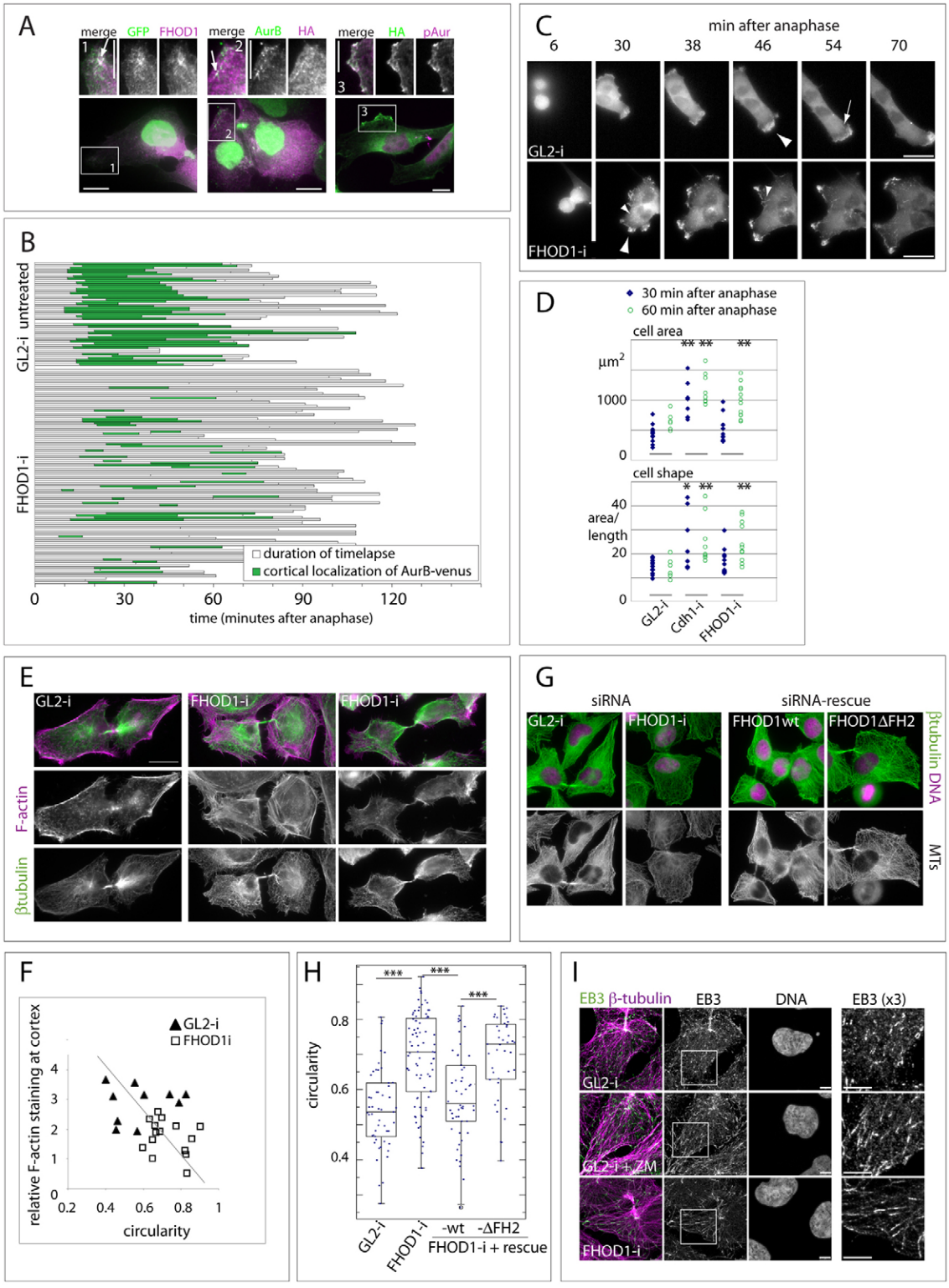

Fig. 3. See next page for legend.

to FHOD1wt, predominantly at sites of colocalisation of MTs with SFs (Fig. 4D–F). HA–FHOD1-5A was less efficient in rescue of SFs and showed a different pattern of localisation. Peripheral SFs were significantly weaker, and polymerized actin was frequently seen extending beyond the MT bundles that usually define the cell edge (Fig. 4D,E). HA–FHOD1-5A, like HA–FHOD1ΔFH2, also showed a reduced tendency to localise with MTs but was observed to colocalise with F-actin along the cell boundaries (Fig. 4D,F). This suggests that AurB-mediated phosphorylation of FHOD1 is required to coordinate the assembly of F-actin fibres with stable oriented MTs at the cell periphery in early G1 phase.

Discussion

We identified a pool of AurB recruited at the cell cortex in early G1 phase that, in contrast to other pools of AurB that undergo phosphatase-mediated inactivation (Steigemann et al., 2009; Wurzenberger et al., 2012) relies exclusively on APC/C-mediated proteolysis for its inactivation at mitotic exit. APC/C^{Cdh1} is required to eliminate most of this pool of AurB, restricting it to protrusions associated with cell spreading and thereby exerting spatial control on the activity of the kinase. We have observed that the duration and size of this pool are sensitive to the surface on which AurB–Venus cells are cultured (N.W. and C.L., unpublished observations) leading us to speculate that AurB could modulate responses to external cues. We are currently working to establish an *in vivo* degradation assay for AurB that will allow us to test whether the rate or timing of AurB proteolysis by APC/C^{Cdh1} is influenced by parameters affecting cell adhesion after division.

Fig. 3. FHOD1 controls AurB localisation and cell spreading during return to interphase. (**A**) AurB–Venus-expressing cells were transfected with HA-tagged FHOD1, fixed and stained after 24 hours with antibodies against FHOD1 and GFP (left-hand panel) or HA and AurB (middle panel). Other cells were treated briefly with MG132 (as in Fig. 1A) and stained for pAur and HA (right-hand panel). Arrows indicate some sites of colocalisation. Scale bars: 10 μm. (**B**) Individual cell trajectories from populations of AurB–Venus cells treated with control or FHOD1 siRNA (supplementary material Movies 7, 8). See also supplementary material Fig. S3. (**C**) Frames from representative movies of RPE-α-actinin–Venus cells filmed as in Fig. 2C after treatment with control or FHOD1 siRNA. Scale bars: 20 μm. (**D**) Time-lapse movies of FHOD1-i RPE-α-actinin–Venus cells were used to calculate cell shape indices as described for Fig. 2E. Gl2-i and Cdh1-i results from Fig. 2E are included for comparison. (**E–I**) U2OS cells synchronized and fixed to optimize staining for F-actin (using phalloidin), for MTs (β-tubulin) or for MT +TIPS (EB3). Cells were treated with control or FHOD1 siRNA, or FHOD1-i together with siRNA-resistant versions of HA-FHOD1 where indicated. Representative images are shown in E, G and I. (F) Values for relative F-actin staining at the cortex in individual cells were calculated as the ratio of maximum value at the cell periphery to average pixel value across the cell (as described in more detail in legend to Fig. 4E) and are plotted here against the circularity measurement for each cell, measured as described in legend to Fig. 3H. Trend line indicates the inverse relationship between peripheral F-actin staining and cell shape. (H) Cell shape measurements were made from images of 40 or more cells acquired from two separate experiments. Circularity is measured on a scale of 0–1, where 1 represents a perfect circle (see Materials and Methods for details). ***$P<0.0001$ by Student's *t*-test. (I) Representative images of cells stained for EB3. ZM was added 15 minutes prior to fixation, where indicated. Images of the boxed regions show regions of the cell edge under increased magnification and contrast, all pixels were treated in an identical fashion. See also supplementary material Fig. S3. Scale bars: 5 μm.

We further identified the formin FHOD1, a known C-phase-specific binding partner (Ozlü et al., 2010), as an essential factor in retaining AurB at the cell cortex. FHOD1 has previously been shown to be an effector of Rac1, with expression of a constitutively active version shown to induce SF assembly, to promote alignment of MTs with SFs, and to enhance cell elongation and migration (Gasteier et al., 2003; Gasteier et al., 2005; Koka et al., 2003). Consistent with this we find phenotypes in FHOD1-knockdown daughter cells that include loss of cell shape and misaligned MTs and SFs, suggesting that FHOD1 plays a specific role in the dynamic interplay between MT and actin cytoskeletons that is required to remodel the shape and polarity of newly divided cells. Our work demonstrates that spatial control of AurB kinase activity by APC/C^{Cdh1} is critical to this remodelling through regulation of targets that include FHOD1. Absence of AurB from the cortex (in FHOD1-i), or else over-recruitment of AurB at the cortex (in Cdh1-i) both lead to loss of cell shape. Therefore we propose that correct cell shape is achieved through stabilization of selected MTs in a manner depending on tightly regulated localisation of AurB. In this scenario, we envision that AurB triggers FHOD1 activity by at least two distinct mechanisms. First, FHOD1 subcellular localisation and activity are regulated by Rac1 (Gasteier et al., 2003; Koka et al., 2003; Westendorf, 2001) and since AurB is an upstream regulator of Rac1 (Bastos et al., 2012; Minoshima et al., 2003), the kinase may indirectly activate FHOD1 via Rac1. Second, we find that a cluster of phosphorylation sites upstream of the FH1 and FH2 domains is phosphorylated by AurB *in vitro*, and that a non-phosphorylatable version of this cluster interferes with the function of FHOD1 in coordinating SF assembly with oriented MTs. We propose that, as in regulation of FHOD1 by ROCK (Hannemann et al., 2008; Takeya et al., 2008), phosphorylation of the DRF by AurB may directly induce conformational changes and/or allow for additional protein interactions. Given the position of AurB phosphorylation sites in FHOD1 near the coiled-coil domain that governs multimerization of the DRF (Madrid et al., 2005), these modifications are likely to affect multimerization rather then autoinhibition of FHOD1. Based on preliminary results indicating decreased multimerization of FHOD1-5D (data not shown), it is tempting to speculate that AurB mediated phosphorylation results in monomeric FHOD1 that is particularly prone to stabilize MTs while FHOD1 without AurB phosphorylation persists as multimer and exclusively acts on actin organization. Further work is required to test this hypothesis and determine the precise properties of FHOD1 regulated by AurB in MT stabilization or actin nucleation.

In our model, active FHOD1 would stabilize a selected population of MTs in FH2 domain-dependent manner, and direct oriented SF assembly at the cell periphery, activities promoted by AurB delivered to the cortex on FHOD1-stabilized MTs (Fig. 5). Our finding that global inhibition of AurB by the kinase inhibitor ZM promoted the appearance of MT plus-ends close to the cell edge suggests, however, that AurB would play a role in destabilizing other MTs at this time in the cell cycle. We reconcile these findings by proposing that alternative binding partners of AurB control distinct populations of MTs. In this model AurB delivered at the cell cortex would either contribute to MT destabilization or, through recruitment by FHOD, to stabilization of selected MTs. APC/C^{Cdh1} would act to restrict the

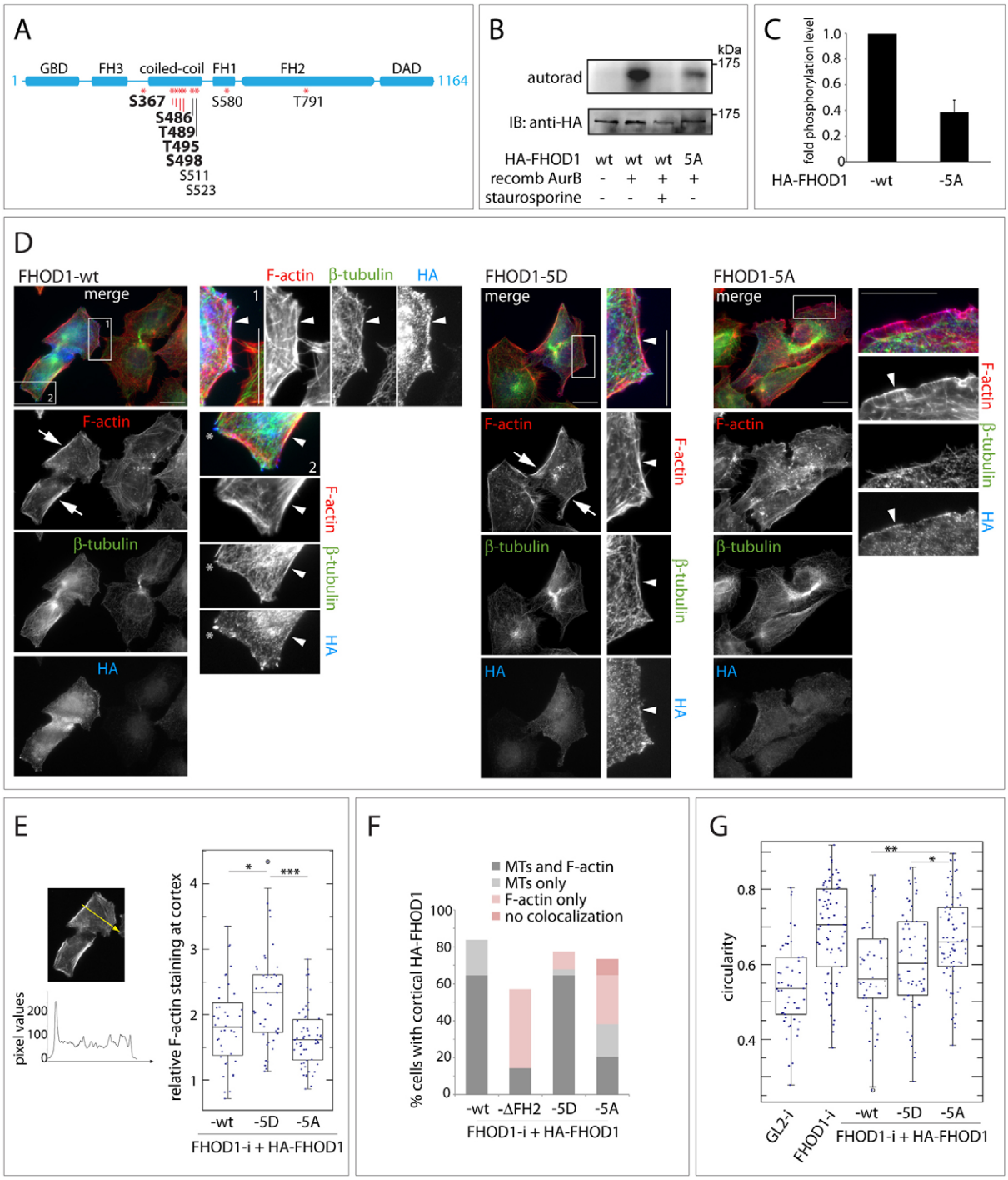

Fig. 4. FHOD1 phosphorylation by AurB coordinates F-actin assembly. (**A**) Schematic of FHOD1 domain organization showing known functional domains and AurB phosphorylation sites identified by mass spectrometry. Further details are in supplementary material Fig. S4. S/T residues in bold were mutated to generate FHOD1-5D and −5A. GBD, GTPase binding domain; DAD, Dia autoregulatory domain; FH, formin homology. (**B**) *In vitro* kinase assay comparing HA–FHOD1wt with HA–FHOD1-5A after immuno-isolation from HEK293T cells and *in vitro* kinase reaction with recombinant AurB. The upper panel depicts an autoradiograph of the kinase reaction, the lower panel an immunoblot to illustrate the amounts of FHOD1 protein in each kinase reaction. (**C**) Quantification of the FHOD1 phosphorylation shown in B. Depicted is the ratio of the phospho-FHOD1 relative to total FHOD1 protein signal, normalized to the values obtained for FHOD1wt (mean of three independent experiments ± s.d.). (**D–G**) U2OS cells were prepared by FHOD1 siRNA-rescue to express different versions of HA–FHOD1, synchronized in early G1 phase and fixed with PFA. (D) Representative images of cells examined for the presence of F-actin, MTs and HA. Arrows indicate prominent F-actin cables at the periphery of daughter cells. Arrowheads in enlarged images indicate sites of colocalisation of labels. Scale bars: 20 µm. (E) F-actin staining was profiled along a cell section (indicated by yellow arrow, left-hand panel) bisecting the direction of maximum spread of daughter cells. Relative staining at the cortex was calculated as the ratio of the maximum value at the cell periphery to average pixel value across the cell. The distribution of data collected from more than 40 cells from two experiments are shown as box-plots. ***$P<0.001$, *$P<0.01$ by Student's *t*-test. (F) Cells from the same experiments were scored for colocalisation of HA–FHOD1 with MTs or SFs at the cell cortex. Bar chart shows percentage of the total number of HA-positive cells examined in different categories. (G) Cell shape analysis was carried out as in Fig. 3G. **$P<0.001$, *$P<0.01$ by Student's *t*-test.

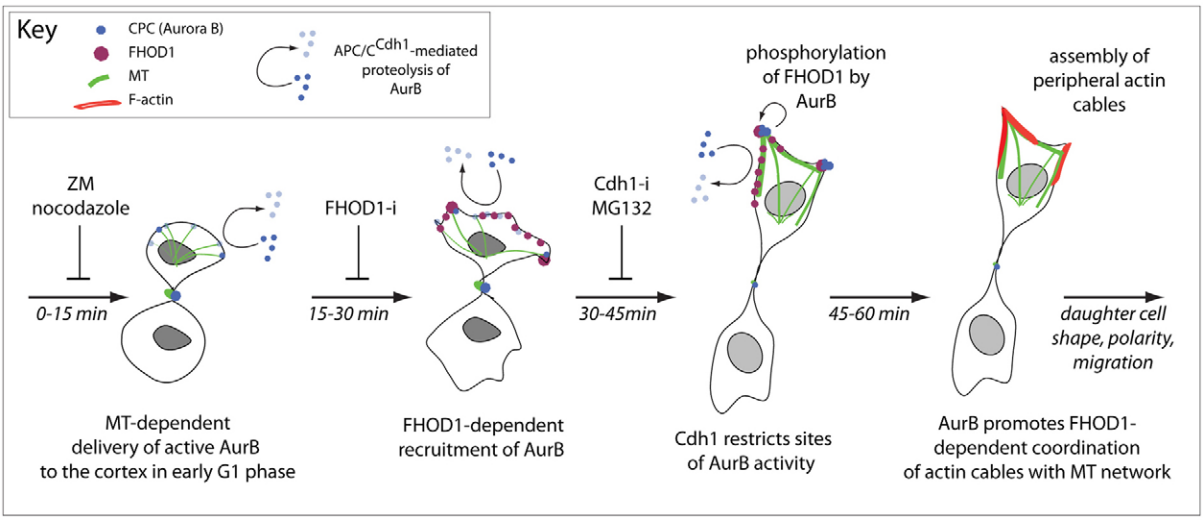

Fig. 5. Proposed model for cell shape control during mitotic exit. Timescales for proposed sequence of events are shown as minutes after anaphase.

pool of AurB activity close to or at the cell cortex to promote polarized cell shape (Fig. 5).

A central role of AurB activity in polarizing events involving both MTs and actin has previously been described during monopolar cytokinesis (Hu et al., 2008), events that we have also found to depend upon FHOD1 (C.M., M.M. and C.L., unpublished data). Coordination of MT and F-actin networks may thus emerge as a central biological property of FHOD1. Understanding further how these components interact with each other both physically and functionally will be critical to understanding how daughter cell identity is established at the beginning of interphase.

Materials and Methods

Plasmids

pTRE-AurB-Venus was made from Aurora B-GFP (kind gift of YL Wang). pEGFP-N1-α-actinin1 (Edlund et al., 2001) was obtained from Addgene and GFP swapped for Venus fluorescent protein to make pVenus-N1-α-actinin. Expression plasmids for HA-FHOD1, HA-FHOD1ΔFH2 were previously described (Gasteier et al., 2003). Expression plasmids for FHOD1-RFP, siRNA-resistant FHOD1 versions, and FHOD1-5D and -5A point mutants were made using standard cloning and site directed mutagenesis techniques and verified by sequencing. Full cloning details for all constructs available on request.

Cell culture, synchronization and transfection

HeLa cells were cultured in high glucose DMEM (Invitrogen, Carlsbad, CA, USA). hTERT-RPE1 (RPE) cells were cultured in 50:50 mix of Ham's F12:DMEM (Sigma-Aldrich, St. Louis, MO, USA). U2OS cells were cultured in 50:50 mix of Leibovitz L15:DMEM. All cell culture media were supplemented with FBS (10%), penicillin–streptomycin and amphotericin B (all from PAA Laboratories, Pasching, Austria). U2OS tet-OFF cell culture medium was additionally supplemented with 500 μg/ml geneticin (PAA) and 1 μg/ml tetracycline hydrochloride (Calbiochem, San Diego, CA, USA).

RPE-α-actinin–Venus cells were made by clonal selection with 500 μg/ml geneticin of cell populations transfected with pVenus-N1-α-actinin-Venus. U2OS-AurB–Venus cells were obtained by clonal selection with 170 μg/ml hygromycin B (Calbiochem) after transfection of U2OS tet-OFF cells with pTRE-AurB-Venus:pCMVhygro in a ratio of 10:1.

HeLa and U2OS cells were synchronized in early G1 phase by release for 13 hours from thymidine/aphidicolin double block. RPE cells were synchronized in early G1 phase by 16 hour release from single thymidine block.

siRNA duplexes targeting sequences in hsCdh1 and hsFHOD1 as previously described (Floyd et al., 2008; Hannemann et al., 2008), and control siRNA duplex against GL2, were obtained from Ambion (Austin, TX, USA).

Transfections were carried out using Lipofectamine® 2000 or Oligofectamine® (Invitrogen). siRNA-rescue experiments were achieved by electroporation using Invitrogen Neon® system to electroporate cells with mixtures of siRNA and siRNA-resistant plasmid, according to the manufacturers' instructions. Cells were analysed 44–48 hours following transfection/electroporation.

Immunofluorescence analysis

Cells were grown on 12 mm glass coverslips, synchronized and fixed using either 100% methanol at −20℃ or 4% PFA treatment at ambient temperature. Full details of buffers, reagents and antibodies used are given in supplementary material Table S1. Widefield images were captured on an Olympus CellR platform (Fig. 1C; Fig. 3A; supplementary material Fig. S1; see description in next section) or an inverted Zeiss Axiovert 200M microscope with 63× 1.3 NA oil objective and CoolSNAP HQ camera (Photometrics, Tucson AZ, USA), running Metamorph® software (Molecular Devices, Sunnyvale, CA, USA; Fig. 1A,E; Fig. 3E,G; Fig. 4D). Confocal images were captured using a TCS SP5 Confocal Leica laser scanning microscope equipped with a DMI60000 microscope and a HCX PL APO Lambda blue 63× 1.4 NA oil objective (Fig. 3I; supplementary material Fig. S3). Intensity level, contrast and brightness of images were adjusted using Adobe Photoshop where indicated.

Pixel quantifications (Fig. 1G; Fig. 3F; Fig. 4E) were carried out in ImageJ, using 16-bit images acquired on widefield microscopes. Circularity calculations (Fig. 3H; Fig. 4G) were carried out in ImageJ, using the equation: $\text{circularity}=4\pi(\text{area}/\text{perimeter}^2)$.

Time-lapse microscopy

Cells were seeded onto 8-well plastic-bottom slides (Ibidi GmbH, Martinsried, Germany) for time-lapse analyses. For both AurB–Venus and α-actinin–Venus experiments cells were seeded at 8×10^4 cm^{-2}. Imaging medium was L-15 supplemented with FBS and antibiotics as described above. Expression of AurB–Venus was induced 24 hours prior to filming, and cells chosen for time-lapse recording according to the presence of a Venus-positive metaphase plate. Dishes were used up to 30 hours after induction, after which AurB–Venus levels were deemed too high (and mitotic aberrations were frequently observed). All time-lapse imaging was carried out on an Olympus CellR imaging platform comprised of Olympus IX81 motorized inverted microscope, Orca CCD camera (Hamamatsu Photonics, Japan), motorized stage (Prior Scientific, Cambridge, UK) and 37℃ incubation chamber (Solent Scientific, Segensworth, UK). Cells were imaged by epifluorescence and DIC microscopy, using appropriate filter sets to record AurB–Venus localisation and α-actinin distribution, using 40× 1.3 NA oil and 60× 1.42 NA oil objectives, respectively. Movies were recorded using Olympus CellR software, as 1 μm stacks of up to 12 fields per experiment, acquired at 2 minute intervals and with 2×2 bin to minimize bleaching. All movies and movie frames are displayed as maximal projections of stacks. Image sequences were analysed using CellR software or else exported as 12-bit tiff files for analysis in ImageJ.

Drug treatments

Cells were subjected to different drug treatments during time-lapse experiments, by addition of drug in a volume not less than 1/100 of the existing dish volume and gentle mixing of medium on the dish using a 1 ml Gilson pipette. Drugs were used at the following final concentrations: MG132 (Tocris Bioscience, Bristol, UK) 4 μM; ZM447439 (Tocris Bioscience) 10 μM; nocodazole (Sigma-Aldrich) 2 μM; taxol (Tocris Bioscience) 5 μM; cytochalasin D (Sigma-Aldrich) 1 μM.

In vitro kinase assays

To assay for phosphorylation by AurB, wt or mutant HA-FHOD1 variants were expressed in HEK293T cells. Following lysis in ROCK lysis buffer [10 mM Tris-HCl, pH 7.5; 40 mM $Na_4P_2O_7 \cdot 10H_2O$; 5 mM EDTA; 150 mM NaCl; 1% (v/v) NP-40; 0.5% (v/v) sodium deoxycholate; 0.025% (v/v) SDS; 1:1000 protease inhibitor cocktail (Roche)], FHOD1 proteins were immuno-isolated with anti-HA antibody (Santa Cruz Biotechnology, Santa Cruz, CA, USA) coupled to protein-G–Sepharose (GE Healthcare, Little Chalfont, UK). After intensive washing in lysis buffer, immunoprecipitates were subjected to kinase reactions in 30 µl kinase assay buffer (5 mM MOPS, pH 7.2; 2.5 mM β-glycerophosphate; 1 mM EGTA; 0.4 mM EDTA; 5 mM $MgCl_2$; 0.5 mM DTT; 1 mM ATP), supplemented with 4 µCi [γ-^{32}P]ATP and with 1 µl recombinant active GST-AurB (Sigma Aldrich) and incubated at 30℃ for 90 minutes. The kinase reaction was inhibited with specific AurB inhibitor ZM447439 or Staurosporine (Sigma Aldrich) where indicated.

For mass spectrometry, the assay was conducted with wild-type full length recombinant FHOD1 [kind gift from Matthias Geyer (Hannemann et al., 2008)] with non-radioactive ATP and 30 minutes incubation at 30℃. Samples were run on an SDS-polyacrylamide gel and stained with Coomassie Brilliant Blue G-250.

Mass spectrometry

For sample preparation, protein bands were manually excised from the gel and tryptic in-gel-digest performed based on the protocol from Rosenfeld (http://www.ncbi.nlm.nih.gov/pubmed/1524213) using modified porcine trypsin, sequencing grade, from Promega (Madison, WI, USA). The collected peptide samples were dried and dissolved in 3% acetonitrile and 0.1% formic acid.

For LC-MS/MS, peptides were separated using a nanoAcquity ultra performance liquid chromatography (UPLC) system (Waters Corporation, Milford, MA, USA) fitted with a trapping (nanoAcquity Symmetry C18.5 µm, 180 µm×20 mm) and an analytical column (nanoAcquity BEH C18, 1.7 µm, 75 µm×200 mm). The outlet of the analytical column was coupled directly to a linear trap quadrupole (LTQ) Orbitrap Velos (Thermo Fisher Scientific, Waltham, MA, USA). Peptides were eluted through the analytical column at a constant flow of 0.3 µl/minute and total runtime 45 minutes. Full scan mass spectrometry spectra with mass range 200–2.000 mass-to-charge ratio (m/z) were acquired in profile mode in the Orbitrap with resolution of 30.000. The most intense ions (up to 15) from the full-scan mass spectrometry were selected for fragmentation in the LTQ. Neutral loss masses for phosphorylations were screened and selected for further fragmentation if present and the multistage activation was enabled.

The raw data were processed using MaxQuant (version 1.0.13.13) (Cox and Mann, 2008), and MS/MS spectra were searched using the Mascot search engine (version 2.2.07, Matrix Science) against a Swissprot database (download 11.07.2012) restricted to human entries, with a maximum of one missed cleavage allowed. Carbamidomethylation was set as fixed modification while methionine oxidation and phosphorylation on S and T were included as variable modifications. The search was performed with an initial mass tolerance of 5 ppm for the precursor ion and 0.5 Da for the MS/MS spectra and a minimum ion score of 20 was applied.

Acknowledgements

We thank Anna Akhmanova for EB3 antibody, Yu-Li Wang for plasmids, Jeroen Krijgsveld and Stefan Leicht (Proteomics Core Facility, EMBL Heidelberg) for MS analysis and Rosa M. Rios for supporting the contribution of M.P.G.

Author contributions

S.F., M.P.G., O.T.F. and C.L. conceived and designed experiments; S.F., N.W., M.P.G., S.K., M.D.L., C.M., M.M., J.W., K.C., and C.L. performed experiments; N.W., M.P.G., S.K., M.D.L., O.T.F., C.L. analysed the data; M.P.G., O.T.F. and C.L. wrote and reviewed the manuscript.

Funding

This work was supported by a Medical Research Council Career Development Award [grant number G120/892 to C.L.]; the Deutsche Forschungsgemeinschaft [grant numbers FA 378/6-2 to O.T.F., GRK1188 fellowship to S.K.]; the Isaac Newton Trust. (to C.L.); a Biochemical Society Summer Studentship (to N.W.); Consolider [grant number CSD2009-00016 to M.P.G.]; and Ministerio de Ciencia e Innovación, Spain, through JdC and Jose Castillejo programs. Deposited in PMC for release after 6 months.

Supplementary material available online at
http://jcs.biologists.org/lookup/suppl/doi:10.1242/jcs.123232/-/DC1

References

Abdullah, A. S., Foong, C. and Murata-Hori, M. (2005). Specific distribution of overexpressed aurora B kinase during interphase of normal epithelial cells. *Cancer Cell Int.* **5**, 31.

Albrecht-Buehler, G. (1977). Daughter 3T3 cells. Are they mirror images of each other? *J. Cell Biol.* **72**, 595-603.

Bartolini, F. and Gundersen, G. G. (2010). Formins and microtubules. *Biochim. Biophys. Acta* **1803**, 164-173.

Bartolini, F., Moseley, J. B., Schmoranzer, J., Cassimeris, L., Goode, B. L. and Gundersen, G. G. (2008). The formin mDia2 stabilizes microtubules independently of its actin nucleation activity. *J. Cell Biol.* **181**, 523-536.

Bastos, R. N., Penate, X., Bates, M., Hammond, D. and Barr, F. A. (2012). CYK4 inhibits Rac1-dependent PAK1 and ARHGEF7 effector pathways during cytokinesis. *J. Cell Biol.* **198**, 865-880.

Capalbo, L., Montembault, E., Takeda, T., Bassi, Z. I., Glover, D. M. and D'Avino, P. P. (2012). The chromosomal passenger complex controls the function of endosomal sorting complex required for transport-III Snf7 proteins during cytokinesis. *Open Biol.* **2**, 120070.

Carmena, M. and Earnshaw, W. C. (2003). The cellular geography of aurora kinases. *Nat. Rev. Mol. Cell Biol.* **4**, 842-854.

Cheng, L., Zhang, J., Ahmad, S., Rozier, L., Yu, H., Deng, H. and Mao, Y. (2011). Aurora B regulates formin mDia3 in achieving metaphase chromosome alignment. *Dev. Cell* **20**, 342-352.

Chesarone, M. A., DuPage, A. G. and Goode, B. L. (2010). Unleashing formins to remodel the actin and microtubule cytoskeletons. *Nat. Rev. Mol. Cell Biol.* **11**, 62-74.

Cimini, D., Wan, X., Hirel, C. B. and Salmon, E. D. (2006). Aurora kinase promotes turnover of kinetochore microtubules to reduce chromosome segregation errors. *Curr. Biol.* **16**, 1711-1718.

Cox, J. and Mann, M. (2008). MaxQuant enables high peptide identification rates, individualized p.p.b.-range mass accuracies and proteome-wide protein quantification. *Nat. Biotechnol.* **26**, 1367-1372.

Ditchfield, C., Johnson, V. L., Tighe, A., Ellston, R., Haworth, C., Johnson, T., Mortlock, A., Keen, N. and Taylor, S. S. (2003). Aurora B couples chromosome alignment with anaphase by targeting BubR1, Mad2, and Cenp-E to kinetochores. *J. Cell Biol.* **161**, 267-280.

Douglas, M. E., Davies, T., Joseph, N. and Mishima, M. (2010). Aurora B and 14-3-3 coordinately regulate clustering of centralspindlin during cytokinesis. *Curr. Biol.* **20**, 927-933.

Edlund, M., Lotano, M. A. and Otey, C. A. (2001). Dynamics of alpha-actinin in focal adhesions and stress fibers visualized with alpha-actinin-green fluorescent protein. *Cell Motil. Cytoskeleton* **48**, 190-200.

Floyd, S., Pines, J. and Lindon, C. (2008). APC/C Cdh1 targets aurora kinase to control reorganization of the mitotic spindle at anaphase. *Curr. Biol.* **18**, 1649-1658.

Gasteier, J. E., Madrid, R., Krautkrämer, E., Schröder, S., Muranyi, W., Benichou, S. and Fackler, O. T. (2003). Activation of the Rac-binding partner FHOD1 induces actin stress fibers via a ROCK-dependent mechanism. *J. Biol. Chem.* **278**, 38902-38912.

Gasteier, J. E., Schroeder, S., Muranyi, W., Madrid, R., Benichou, S. and Fackler, O. T. (2005). FHOD1 coordinates actin filament and microtubule alignment to mediate cell elongation. *Exp. Cell Res.* **306**, 192-202.

Hannemann, S., Madrid, R., Stastna, J., Kitzing, T., Gasteier, J., Schönichen, A., Bouchet, J., Jimenez, A., Geyer, M., Grosse, R. et al. (2008). The Diaphanous-related Formin FHOD1 associates with ROCK1 and promotes Src-dependent plasma membrane blebbing. *J. Biol. Chem.* **283**, 27891-27903.

Hu, C. K., Coughlin, M., Field, C. M. and Mitchison, T. J. (2008). Cell polarization during monopolar cytokinesis. *J. Cell Biol.* **181**, 195-202.

Hümmer, S. and Mayer, T. U. (2009). Cdk1 negatively regulates midzone localization of the mitotic kinesin Mklp2 and the chromosomal passenger complex. *Curr. Biol.* **19**, 607-612.

Kettenbach, A. N., Schweppe, D. K., Faherty, B. K., Pechenick, D., Pletnev, A. A. and Gerber, S. A. (2011). Quantitative phosphoproteomics identifies substrates and functional modules of Aurora and Polo-like kinase activities in mitotic cells. *Sci. Signal.* **4**, rs5.

Knowlton, A. L., Lan, W. and Stukenberg, P. T. (2006). Aurora B is enriched at merotelic attachment sites, where it regulates MCAK. *Curr. Biol.* **16**, 1705-1710.

Koka, S., Neudauer, C. L., Li, X., Lewis, R. E., McCarthy, J. B. and Westendorf, J. J. (2003). The formin-homology-domain-containing protein FHOD1 enhances cell migration. *J. Cell Sci.* **116**, 1745-1755.

Kunda, P. and Baum, B. (2009). The actin cytoskeleton in spindle assembly and positioning. *Trends Cell Biol.* **19**, 174-179.

Lindon, C. (2008). Control of mitotic exit and cytokinesis by the APC/C. *Biochem. Soc. Trans.* **36**, 405-410.

Lindon, C. and Pines, J. (2004). Ordered proteolysis in anaphase inactivates Plk1 to contribute to proper mitotic exit in human cells. *J. Cell Biol.* **164**, 233-241.

Liot, C., Seguin, L., Siret, A., Crouin, C., Schmidt, S. and Bertoglio, J. (2011). APC(cdh1) mediates degradation of the oncogenic Rho-GEF Ect2 after mitosis. *PLoS ONE* **6**, e23676.

Madrid, R., Gasteier, J. E., Bouchet, J., Schröder, S., Geyer, M., Benichou, S. and Fackler, O. T. (2005). Oligomerization of the diaphanous-related formin FHOD1 requires a coiled-coil motif critical for its cytoskeletal and transcriptional activities. *FEBS Lett.* **579**, 441-448.

Minoshima, Y., Kawashima, T., Hirose, K., Tonozuka, Y., Kawajiri, A., Bao, Y. C., Deng, X., Tatsuka, M., Narumiya, S., May, W. S., Jr et al. (2003). Phosphorylation

by aurora B converts MgcRacGAP to a RhoGAP during cytokinesis. *Dev. Cell* **4**, 549-560.

Murnion, M. E., Adams, R. R., Callister, D. M., Allis, C. D., Earnshaw, W. C. and Swedlow, J. R. (2001). Chromatin-associated protein phosphatase 1 regulates aurora-B and histone H3 phosphorylation. *J. Biol. Chem.* **276**, 26656-26665.

Naoe, H., Araki, K., Nagano, O., Kobayashi, Y., Ishizawa, J., Chiyoda, T., Shimizu, T., Yamamura, K., Sasaki, Y., Saya, H. et al. (2010). The anaphase-promoting complex/cyclosome activator Cdh1 modulates Rho GTPase by targeting p190 RhoGAP for degradation. *Mol. Cell. Biol.* **30**, 3994-4005.

Neef, R., Klein, U. R., Kopajtich, R. and Barr, F. A. (2006). Cooperation between mitotic kinesins controls the late stages of cytokinesis. *Curr. Biol.* **16**, 301-307.

Nguyen, H. G., Chinnappan, D., Urano, T. and Ravid, K. (2005). Mechanism of Aurora-B degradation and its dependency on intact KEN and A-boxes: identification of an aneuploidy-promoting property. *Mol. Cell. Biol.* **25**, 4977-4992.

Ozlü, N., Monigatti, F., Renard, B. Y., Field, C. M., Steen, H., Mitchison, T. J. and Steen, J. J. (2010). Binding partner switching on microtubules and aurora-B in the mitosis to cytokinesis transition. *Mol. Cell. Proteomics* **9**, 336-350.

Picone, R., Ren, X., Ivanovitch, K. D., Clarke, J. D., McKendry, R. A. and Baum, B. (2010). A polarised population of dynamic microtubules mediates homeostatic length control in animal cells. *PLoS Biol.* **8**, e1000542.

Pines, J. (2011). Cubism and the cell cycle: the many faces of the APC/C. *Nat. Rev. Mol. Cell Biol.* **12**, 427-438.

Ramadan, K., Bruderer, R., Spiga, F. M., Popp, O., Baur, T., Gotta, M. and Meyer, H. H. (2007). Cdc48/p97 promotes reformation of the nucleus by extracting the kinase Aurora B from chromatin. *Nature* **450**, 1258-1262.

Sigl, R., Wandke, C., Rauch, V., Kirk, J., Hunt, T. and Geley, S. (2009). Loss of the mammalian APC/C activator FZR1 shortens G1 and lengthens S phase but has little effect on exit from mitosis. *J. Cell Sci.* **122**, 4208-4217.

Steigemann, P., Wurzenberger, C., Schmitz, M. H., Held, M., Guizetti, J., Maar, S. and Gerlich, D. W. (2009). Aurora B-mediated abscission checkpoint protects against tetraploidization. *Cell* **136**, 473-484.

Stewart, S. and Fang, G. (2005). Destruction box-dependent degradation of aurora B is mediated by the anaphase-promoting complex/cyclosome and Cdh1. *Cancer Res.* **65**, 8730-8735.

Sumara, I., Quadroni, M., Frei, C., Olma, M. H., Sumara, G., Ricci, R. and Peter, M. (2007). A Cul3-based E3 ligase removes Aurora B from mitotic chromosomes, regulating mitotic progression and completion of cytokinesis in human cells. *Dev. Cell* **12**, 887-900.

Takeya, R., Taniguchi, K., Narumiya, S. and Sumimoto, H. (2008). The mammalian formin FHOD1 is activated through phosphorylation by ROCK and mediates thrombin-induced stress fibre formation in endothelial cells. *EMBO J.* **27**, 618-628.

Vagnarelli, P., Ribeiro, S., Sennels, L., Sanchez-Pulido, L., de Lima Alves, F., Verheyen, T., Kelly, D. A., Ponting, C. P., Rappsilber, J. and Earnshaw, W. C. (2011). Repo-Man coordinates chromosomal reorganization with nuclear envelope reassembly during mitotic exit. *Dev. Cell* **21**, 328-342.

Vázquez-Novelle, M. D. and Petronczki, M. (2010). Relocation of the chromosomal passenger complex prevents mitotic checkpoint engagement at anaphase. *Curr. Biol.* **20**, 1402-1407.

Westendorf, J. J. (2001). The formin/diaphanous-related protein, FHOS, interacts with Rac1 and activates transcription from the serum response element. *J. Biol. Chem.* **276**, 46453-46459.

Wurzenberger, C. and Gerlich, D. W. (2011). Phosphatases: providing safe passage through mitotic exit. *Nat. Rev. Mol. Cell Biol.* **12**, 469-482.

Wurzenberger, C., Held, M., Lampson, M. A., Poser, I., Hyman, A. A. and Gerlich, D. W. (2012). Sds22 and Repo-Man stabilize chromosome segregation by counteracting Aurora B on anaphase kinetochores. *J. Cell Biol.* **198**, 173-183.